



**HAL**  
open science

## Effect of operating parameters on a centrifugal partition chromatography separation

Norbert Fumat, Alain Berthod, Karine Faure

► **To cite this version:**

Norbert Fumat, Alain Berthod, Karine Faure. Effect of operating parameters on a centrifugal partition chromatography separation. *Journal of Chromatography A*, 2016, 1474, pp.47-58. 10.1016/j.chroma.2016.10.014 . hal-01515264

**HAL Id: hal-01515264**

**<https://hal.science/hal-01515264v1>**

Submitted on 23 Jul 2020

**HAL** is a multi-disciplinary open access archive for the deposit and dissemination of scientific research documents, whether they are published or not. The documents may come from teaching and research institutions in France or abroad, or from public or private research centers.

L'archive ouverte pluridisciplinaire **HAL**, est destinée au dépôt et à la diffusion de documents scientifiques de niveau recherche, publiés ou non, émanant des établissements d'enseignement et de recherche français ou étrangers, des laboratoires publics ou privés.

# Effect of operating parameters on a Centrifugal Partition Chromatography separation

Norbert Fumat, Alain Berthod, Karine Faure\*

*Univ Lyon, CNRS, Université Claude Bernard Lyon 1, Ens de Lyon, Institut des Sciences Analytiques, UMR 5280, 5 rue de la Doua, F-69100 Villeurbanne, France*

## Abstract

Centrifugal partition chromatography (CPC) is the branch of countercurrent chromatography (CCC) that works with single axis hydrostatic columns with rotary seals. The hydrodynamic of the liquid stationary phase-liquid mobile phase equilibrium in the CPC chambers has been studied theoretically and with specially designed CPC columns. In this work, we selected a simple analytical separation (no loading study) of three test solutes, coccine red, coumarin and carvone, with a commonly used heptane/ethyl acetate/methanol/water 1:1:1:1 v/v biphasic liquid system and two different rotors: a commercially available 30-mL CPC instrument and a 80-mL prototype rotor designed for productivity. We fully studied this separation in many possible practical operating conditions of the two rotors, aiming at a generic column characterization. The rotor rotation was varied between 1000 and 2800 rpm, the aqueous mobile phase flow rate was varied between 1 and 22 mL/min with the 30-mL rotor and 10 and 55 mL/min with the 80-mL rotor, the upper limits being mechanical constraints and some liquid stationary phase remaining in the rotor. The variations of  $S_f$ , the volume ratio of stationary phase in the rotor, were studied versus mobile phase flow rate and rotor rotation speed. A maximum mobile phase linear velocity was found to depend on the centrifugal field for the 30-mL rotor. This maximum velocity was not observed with the 80-mL rotor. Studying the changes in coumarin and carvone peak efficiencies, it is established that the number of cells required to make one theoretical plate, i.e. one chromatographic exchange, is minimized at maximal rotation speed and, to a lesser extent, at high mobile phase flow rate (or linear velocity). Considering the throughput, there is evidence of an optimal flow rate depending on the rotor rotation that is not necessarily the highest possible.

## Keywords

Centrifugal partition chromatography, countercurrent chromatography, stationary phase retention, mobile phase velocity, efficiency, productivity.

## Highlights

- Practical study of stationary phase retention versus mobile phase flow rate,
- Effect of the centrifugal field strength (rotor rotation),
- Effect of flow rate and field strength on peak efficiencies,
- Optimization of preparative productivity.

---

\* To whom all correspondance should be sent: [karine.faure@isa-lyon.fr](mailto:karine.faure@isa-lyon.fr)

41

## 42 1. Introduction

43

44 Countercurrent chromatography (CCC) is a separation technique that uses two liquid  
45 phases without solid support. Two main advantages compensate for the need of a centrifugal  
46 field to hold the liquid stationary phase steady while the liquid mobile phase percolates  
47 through it [1-3]. The first advantage is the high load possible in the volume of the liquid  
48 stationary phase compared to the overload problems commonly encountered with saturated  
49 surfaces of solid stationary phases. The second advantage is that CCC offers a huge selectivity  
50 panel since chemists can finely tune their solvent system to the sample to be purified.  
51 Solvent selection in CCC is crucial since it is selecting at the same time the stationary phase,  
52 which would be the column in other chromatographic techniques, and the mobile phase. Any  
53 composition change in one liquid phase may induce a change in the other liquid phase. To  
54 help in the delicate and time-consuming step of liquid system selection in CCC, databases  
55 now gather the literature worldwide experience [4, 5].

56 Two types of CCC columns were made commercially available: i) the hydrodynamic CCC  
57 columns with rotating coils of simple tubing and ii) the hydrostatic CCC columns called  
58 Centrifugal Partition Chromatographs (CPC) with disks of interconnected cells. A great deal  
59 of efforts have been carried out since the past 10 years by suppliers to provide robust and  
60 efficient technologies, for both hydrodynamic CCC and hydrostatic CPC instruments.  
61 However, it is still not rare to encounter users complaining about long runs (hours) and  
62 broad peaks when working with CCC columns. This common observation comes from the  
63 fact that, while spending days to work on selectivity finely tuning the liquid system for the  
64 purification, the instrument operating parameters are overlooked and not optimized, leading  
65 to a false image of CCC and discouraging beginners. In 2005, Ito provided general rules for  
66 hydrodynamic CCC instruments [6]. In this work, we would like to study how the CPC  
67 operating parameters are related to throughput with a simple analytical separation. The  
68 numerous problems associated with large mass and/or volume injections were not examined.

69 In CPC, the two main concerns are i) stationary phase retention, that influences retention  
70 volumes and hence resolution as well as time- and solvent-consumption, and ii) band  
71 broadening, related to peak sharpness, peak overlaps, resolution and final purity of the  
72 collected fractions. A special parameter,  $S_f$ , has to be introduced in CCC which describes  
73 variable stationary phase volumes [1-3].  $S_f$  is defined as the ratio of  $V_s$ , the volume of  
74 stationary phase over  $V_c$ , the column volume. Two groups have extensively worked on  $S_f$  and  
75 band broadening in CPC. The group of Marchal from St Nazaire (France) developed an  
76 impressive work on mass transfer and flow regimes based on visualization using a specially  
77 designed CPC instrument with a transparent disk. They modeled mass transfer and  
78 efficiencies and proposed improvements of cell design [7-9]. Introducing the concept of  
79 height of a transfer unit (HTU), they established that increasing both centrifugal field and  
80 flow rate improved mixing, interfacial area and hence mass transfer. Schembecker at  
81 Dortmund (Germany) also used flow visualization to study flow patterns in a transparent disk  
82 CPC working with various solvent systems and comparing different cell designs. This group  
83 pointed out the impact of phase viscosity on stationary phase retention [10-12]. While  
84 suggesting improvements on cell design and a preferential selection of solvent systems with  
85 low interfacial tension, their advice on operating parameters is limited to the use of maximal  
86 rotation speed.

87 While these two groups provided a work of tremendous quality in understanding the  
88 effect of operating parameters on hydrodynamics, their main purpose remained CPC cell  
89 engineering and their tools, such as flow visualization instruments and mathematical models,  
90 seem only accessible to experts.

91 Our purpose is to confirm the general trends that were previously exposed and practically  
92 observed in CPC practice. The systematic study is based on a simple separation of standards  
93 working with two different commercial CPC instruments at low concentration. The influence  
94 of the mobile phase flow rate and rotor rotation speed (centrifugal field) on stationary phase  
95 retention, band broadening, resolution and throughput will be experimentally studied with  
96 these two different rotors and the same test solute sample (low concentration) and liquid  
97 system.

98

99

## 100 **2. Experimental section**

101

### 102 *2.1 Apparatus*

103

104 The frame instrument is a hydrostatic apparatus model, FCPC-A from Kromaton  
105 Rousselet-Robatel (Annonay, France) including safety casing, motor with its electronic  
106 regulation and a fan with a liquid cooling circulation. Its central shaft can receive  
107 interchangeable columns (or rotors). Two 32-cm diameter rotors were used. The first one is  
108 a commercially available rotor. It had a measured exact volume of 33.25 mL with 832 twin-  
109 cells with a number-eight shape at an average distance of 10 cm from the central axis of  
110 rotation. The Kromaton Company proposed to test a prototype rotor of larger volume  
111 designed for preparative purification at high flow rates. The prototype rotor has an exact  
112 volume measured as 83.4 mL with 406 twin-cells also at an average distance of 10 cm of the  
113 central axis. The exact shape of the cell is proprietary. The rotor could fit into the FCPC-A  
114 frame. All known characteristics of the two rotors are listed in Table 1. For convenience, the  
115 analytical and preparative rotors will be referred as the 30-mL and 80-mL rotors,  
116 respectively.

117 A refrigerated circulator F10-C Julabo (Colmar, France) was used to cool down the CPC  
118 instrument by flowing chilled water in the dedicated lines of the FCPC-A frame. A Puriflash  
119 integrated system from Interchim (Montluçon, France) was used for solvent delivery,  
120 injection and detection. This equipment is the assembly of a quaternary pump (flow rate  
121 from 1 to 60 mL/min, maximal pressure 200 bar), an automatic loop injection valve fitted  
122 with a 10 mL sample loop, a UV/VIS dual wavelength spectrophotometer set at 254 nm and  
123 280 nm and a fraction collector. An integrated computer with touch-screen allows for full  
124 apparatus control and data acquisition.

125 The volume of connecting tubing or extra-rotor volume has been measured to be 4.9 mL  
126 from injection to detection points.

### 127 *2.2 Phase system and test solutes*

128 All reagents were of analytical grade. Methanol, heptane and ethyl acetate as well as the  
129 three model solutes new coccine red, coumarin and carvone were purchased from Sigma-  
130 Aldrich (Saint-Quentin Fallavier, France).

131 The selected solvent system on all experiments was the heptane/ethyl  
132 acetate/methanol/water 1:1:1:1 (v/v) mixture also referred as Arizona N or HEMWat zero  
133 system [13]. After full equilibration, one liter of this solvent system splits at room  
134 temperature in two phases: 412 mL of the upper phase with heptane, ethyl acetate, methanol  
135 and water composition 62.5/34.4/2.6/0.5 % v/v, density 0.752 g/mL, viscosity 0.40 cP or  
136 mPa.s, and 588 mL of lower phase with 0.1/18.3/39.9/41.7 %v/v, density 0.898 g/mL,  
137 viscosity 1.45 cP or mPa.s. The phase density difference is 0.146 g/mL and the interfacial  
138 tension is 2.5 mN/m [11, 13]. With the relatively polar test solutes selected, this solvent  
139 system was used in the reversed phase mode i.e. the mobile phase was the aqueous polar  
140 lower phase flown in the descending mode. The liquid stationary phase was the less polar  
141 organic upper phase.

142 The test solutes selected to carry on the study were picked up from the solute list  
143 proposed by Friesen and Pauli [14, 15]. The selection was based on UV absorptivity and a  
144 wide polarity range implying a large range of partition coefficients in very different liquid  
145 systems. New coccine red is a charged compound that did not partition in the selected  
146 solvent system being exclusively located in the aqueous lower phase coloring it red. It was  
147 therefore used as a non-retained marker for mobile phase volume determination. Coumarin  
148 and carvone were selected with partition coefficient of  $1.3 \pm 0.3$  and  $7.5 \pm 0.5$ , respectively, in  
149 the 1:1:1:1 Arizona N or HEMWat o system. Coumarin spends as much time in the stationary  
150 organic phase as in the aqueous mobile phase of this system. Carvone favors the less polar  
151 stationary phase of the selected liquid system: it is a compound that exhibits a high retention  
152 factor in the selected solvent system. Resolution and efficiency will be studied with  
153 coumarin and carvone even at very low stationary phase retention volume ratio.

154

### 155 2.3 *Experimental procedure*

156 The rotor to be used, either the 30-mL standard rotor or the 80-mL prototype rotor, was  
157 installed inside the FCPC-A frame, connected to the upper and lower rotary seals and rinsed  
158 first with the lower phase and next with the upper phase of the HEMWat o (or AZ N) solvent  
159 system. The cooling unit was set to circulate water at 15°C to remove calories out of the  
160 FCPC-A chamber whose temperature would otherwise rise due to heat generated by rotary  
161 seal rotation. With the rotor spinning at 2500 rpm, the FCPC-A chamber temperature was  
162 monitored stable at 21°C.

163 For a given experiment, the rotor spinning at 600 rpm is entirely filled with the upper  
164 stationary phase at 5 mL/min (30-mL rotor) or 15 mL/min (80-mL rotor) in the descending  
165 mode. Then the rotation is set up at the speed needed for the experiment. Table 2 indicates  
166 the relationship between centrifugal fields and rotation speeds for the two rotors with cells at  
167 an average 10 cm distance from the central axis. After the working rotational speed is  
168 stabilized (less than 2 min), the lower aqueous mobile phase is pumped through the  
169 stationary phase in the descending mode. The driving pressure is monitored increasing as  
170 more cells are equilibrated and only upper organic phase is collected at the column exit. As  
171 the pressure reaches its maximal value during equilibration, the maximum pressure security  
172 electronic switch is set at 70 bars to protect the rotary seals. The equilibrium is reached when  
173 the driving pressure stabilizes and only the lower mobile phase is collected exiting the

174 column and the UV signals (254 and 280 nm) stabilize on their respective baseline. In our  
175 solvent system, the existence of a void volume marker allowed the calculation of the  
176 stationary phase volume. But it is also possible to collect the displaced stationary phase  
177 volume and to deduce from this collected phase the volume of stationary phase remaining in  
178 the column. This method is however less accurate than the void volume marker. All extra  
179 volumes have to be carefully taken into account, especially that from the pumping system to  
180 the injection point and from the detection cell to the collection point.

181 Analytical injections consisted in the injection of a sample volume not higher than 2%  
182 column volume and a low sample concentration giving a signal/noise ratio  $\geq 10$ . In this way,  
183 the peaks have Gaussian appearance (Fig. 1). The analytical conditions were 0.5 mg/mL new  
184 coccine red, 1.5 mg/mL coumarin and 2.5 mg/mL carvone with an injection volume of 0.5  
185 mL corresponding to 1.5% and 0.6% of the 30-mL and 80-mL rotors, respectively. In these  
186 injection conditions, the contribution of the dispersion in injection loop can be neglected in  
187 regards to chromatographic dispersion.

188

#### 189 2.4 Data acquisition and theory

190 The stationary phase volume ( $V_S$ ) is deduced using the mobile phase volume ( $V_M$ ),  
191 experimentally obtained as the unretained new coccine red elution volume. This  
192 experimental mobile phase volume includes the mobile phase contained in the rotor and the  
193 mobile phase contained in the extra-column volume (4.9 mL). *Sf*, the stationary phase  
194 retention volume ratio discussed in this study, corresponds to the ratio of  $V_S$ , the amount of  
195 stationary phase contained in the rotor, over  $V_C$ , the rotor volume. Since it is assumed that  
196 the chromatographic extra-volume (injection loop, connecting tubing and detection cell) are  
197 entirely filled with mobile phase, the  $V_S$  volume will be taken as  $V_S = (V_C + 4.9) - V'_M$ , with  $V_C$   
198 being either 33.25 (30-mL rotor) or 83.4 (80-mL rotor) and  $V'_M$  being the coccine red  
199 retention volume.

200 The Azur software (Datalys, France) provides peak retention time, peak width at half-  
201 height expressed in time unit. The peak standard deviation,  $\sigma_{obs}$  is back calculated through  
202 eq. 1, where  $w_{0.5}$  is the peak width at half height.

$$203 \quad \sigma_{obs} = \frac{w_{0.5}}{2.354} \quad \text{eq. 1}$$

204  $\sigma_{obs}$  can also be related to the peak width expressed as  $2 \sigma_{obs}$  at 60% of peak height or  $4 \sigma_{obs}$  at  
205 peak base when the peak is fully Gaussian.

206 The peak standard deviation  $\sigma_{tubing}$  occurring in connecting tubing is quantified using the  
207 same equation when replacing the rotor by a zero-dead-volume connector and injecting a  
208 tracer.

209 In the Gauss theory, the peak standard deviation  $\sigma$  relates to the peak width (eq 1), while  
210 the peak variance  $\sigma^2$  relates to the physical phenomenon that cause this band broadening.  
211 Since the solute band spreads through various dispersion effects, the variances  $\sigma^2$  are  
212 additives. Hence, the dispersion due to the rotor  $\sigma^2_{rotor}$ , is deduced from the variance  
213 obtained from the overall separation,  $\sigma^2_{obs}$ , minus  $\sigma^2_{tubing}$ , the tubing variance (eq. 2).

214

$$215 \quad \sigma^2_{rotor} = \sigma^2_{obs} - \sigma^2_{tubing} \quad \text{eq. 2}$$

216

217 The effective number of theoretical plate generated in the rotor is hence calculated  
218 through eq. 3.

$$219 \quad N_{effective} = \frac{(V_r - V_{extra-column})^2}{\sigma_{rotor}^2} \quad eq. 3$$

220 By analogy with the height equivalent to a theoretical plate, we introduce the number of  
221 cells required to make one theoretical plate ( $NC/TP$ ) defined as eq.4, with  $n_c$  being 832 cells  
222 (30-mL rotor) or 406 cells (80-mL rotor).

$$223 \quad NC / TP = \frac{n_c}{N_{effective}} \quad eq.4$$

224

225 The resolution factor between two adjacent peaks 1 and 2,  $R_s$ , is defined as the distance  
226 between peak apexes divided by the average peak base width  $[(W_1 + W_2)/2]$ .  $R_s$  is calculated  
227 using eq. 5 for a fully Gaussian peak:

228

$$229 \quad R_s = \frac{V_{R2} - V_{R1}}{2(\sigma_2 + \sigma_1)} \quad eq. 5$$

230

## 231 2.5 Reproducibility

232 Five analytical injections of the test mixture were done with newly equilibrated 30-mL  
233 rotor with the same batch of Arizona N system for five successive days. The rotor spinning  
234 was 2500 rpm (712 g) and the mobile phase flow rate 9 mL/min. The relative standard  
235 deviations were 2.6% for  $S_f$ , the stationary phase retention volume ratio, 2.9% for the  
236 coumarin dispersion, 2.1% for carvone dispersion and 1.0% for the  $R_s$  resolution factor. This  
237 reproducibility was acceptable so that, for routine control, repeated injections were  
238 intermittently and randomly performed unless, for any reason, it was found necessary.

239 It was feared that ethyl acetate could hydrolyze in ethanol and acetic acid upon standing  
240 after the Arizona N (HEMWat O) mixture was prepared. To ensure that the liquid biphasic  
241 system was stable in temperature and chemical composition, the partition coefficients of the  
242 two retained compounds were monitored at all time. The coumarin and carvone  $K$  values  
243 were respectively  $1.3 \pm 0.2$  and  $7.5 \pm 0.4$ , with the standard deviations being calculated for 67  
244 experiments obtained working at 5 different centrifugal fields over four months. This test  
245 shows the high reproducibility of the CPC experiments over a long period. Ethyl acetate is  
246 mainly located in the upper phase of the selected HEMWat O (AZ N) system where it cannot  
247 hydrolyze due to water scarcity. In the aqueous lower phase, the ester hydrolysis seems  
248 hindered by the high methanol concentration (40% v/v). No pH change of the aqueous lower  
249 phase was noted over two weeks that was however the maximum time that we set for use of a  
250 particular batch of HEMWat O (AZ N) mixture.

251

252

### 253 3. Results and discussion

254

255 Modern CCC columns have a significantly better capability to retain liquid stationary  
256 phases than first generation instruments. Since CCC is a preparative technique, the CCC  
257 columns must be used to produce a maximum of purified compounds as quickly as possible  
258 and using the least possible solvents. In this work, the 30-mL CPC rotor will be used to study  
259 liquid stationary phase retention through the variation of  $Sf$  within the whole range of  
260 operating parameters. The 80-mL rotor designed for preparative separations will be  
261 similarly tested focusing on high flow rates and rotation speeds. Fig. 1 is the only set of  
262 chromatograms shown. Since the same test mixture was used all over this work, all  
263 chromatograms look alike. The peak retention times change as illustrated by the two very  
264 different conditions of the two Fig. 1 chromatograms whose full details are listed in Table 3 as  
265 an example.

266

#### 267 3.1. Liquid stationary phase retention

268 In hydrodynamic CCC instruments, it was demonstrated that the column acted like a  
269 constant-pressure drop pump, the stationary phase retention volume ratio  $Sf$  decreases  
270 linearly with the square root of flow rate [16] and in a more complex manner  $Sf$  depends on  
271 rotor rotation (centrifugal field) and especially tubing bore [17]. With the accurate  
272 knowledge of stationary phase retention over a wide range of operating conditions, it is  
273 possible to predict peak retention volumes and elution times.

274 In hydrostatic (CPC) instruments, the stationary phase retention,  $Sf$ , does not follow the  
275 same equations. The first studies of  $Sf$  evolution in CPC found a direct decrease in  $Sf$  values  
276 with increasing flow rates,  $F$ . The slope of the  $Sf$  versus  $F$  lines was not dependent on the  
277 centrifugal field for rotor rotation higher than 800 rpm [18, 19]. The intercept of the  $Sf$   
278 versus  $F$  lines corresponded to the connecting duct volume containing only the mobile phase  
279 [18]. Later studies confirmed this trend sometimes finding change in the slope of the  $Sf$   
280 versus  $F$  lines at higher flow rates [11, 20, 21].

281

282

#### 283 *Sf versus flow rate studies*

284

285 The HEMWat o (Arizona N) organic upper phase retention volume ratio was monitored  
286 at different flow rates of the aqueous lower phase in the 30-mL rotor for 5 different  
287 centrifugal fields (or forces) ranging from 112  $g$  to 882  $g$ , i.e. rotor rotation between 1000  
288 rpm and 2800 rpm, Table 2 (Fig. 2A). As expected,  $Sf$ , the stationary phase retention  
289 volume ratio decreases when the mobile phase flow rate increases. However, the linear trend  
290 was not observed at any studied field and the shapes of our  $Sf$  versus flow rate  $F$  curves differ  
291 somewhat from those obtained in similar studies [9, 12]. Taking in account that the rotary  
292 seals of our CPC unit were generating a significant amount of heat, we propose two  
293 explanations for the observed shapes of the  $Sf$  versus  $F$  curves for the 30-mL rotor (Fig. 2A).

- 294 • At moderate centrifugal force below 400  $g$ , i.e. rotor rotation lower than 2000 rpm, the  
295 cooling external circulation could eliminate enough calories so that the CPC entrance was

296 not heated.  $Sf$  decreases linearly with low flow rates as previously described [11, 18-21].  
297 At a certain flow rate depending on the applied centrifugal force, a change of slope is  
298 observed. At 1000 rpm, with a centrifugal force of 112  $g$ , the initial slope is -  
299 2.8%/(mL/min) up to 7 mL/min. At flow rates higher than 7 mL/min, the slope becomes  
300 -6.3%/(mL/min). It means that the first 7 mL/min flow rate produced a  $Sf$  reduction of  
301 19.6%. However, further increasing the flow rate of the same amount, from 7 mL/min ( $Sf$   
302 = 54%) to 14 mL/min ( $Sf = 10\%$ ), drastically reduces the  $Sf$  factor by more than 82% (Fig.  
303 2A).

304 At 1800 rpm, the centrifugal force is three times higher: 365  $g$ , the initial slope is also -  
305 2.8%/(mL/min) but keeping it up to 13 mL/min. At flow rates higher than 13 mL/min,  
306 the slope becomes -5%/(mL/min). A similar behavior was observed at 1000 rpm.

307 In previous CPC columns, flooding was observed at low rotation speed [18, 22-23]. In  
308 flooding conditions, there is a continuous leak of liquid stationary phase up to the point  
309 where it is all washed out with  $Sf = 0$ . In our case, we observe a change in slope of the  $Sf$   
310 versus  $F$  lines. The stationary phase  $Sf$  is lower than expected but still reproducible and  
311 stable over the experiment duration: there is no uninterrupted flooding.

- 312 • At high centrifugal force, i.e. rotor rotation higher than 2000 rpm, we suspect that the  
313 cooling circulating liquid was not able to completely eliminate the calories generated by  
314 the rotary seals. The entering mobile phase was heated by the rotary seal which changed  
315 the mutual solubility between the two phases of the HEMWat o (AZ N) system and  
316 completely disrupted the equilibrium at column entrance producing a lower than  
317 expected  $Sf$  value. As the mobile phase flow rate increases, the mobile phase itself acts as  
318 a cooling agent and the observed  $Sf$  becomes closer to the expected value (dotted line in  
319 Fig. 2A). Here also, it is important to note that the obtained  $Sf$  values were reproducible.

320

### 321 *Average linear mobile phase velocity*

322

323 In HPLC, the linear mobile phase velocity is an important parameter allowing to compare  
324 results obtained with columns of different diameters and lengths. Assuming that the CPC  
325 column can be considered as a homogeneous tube of average cross sectional area  $A_C$ , it will be  
326 possible to calculate an average linear mobile phase velocity,  $u$ , as the ratio of the flow rate,  $F$ ,  
327 over  $A_C$ . It should be considered however that the liquid stationary phase occupies part of the  
328 CPC column so that the velocity,  $u$ , should be computed using the  $Sf$  factor as:

$$329 \quad u = \frac{F}{A_C (1 - Sf)} \quad \text{eq. 6}$$

330

331 The average cross section of the 30-mL rotor was given by the Kromaton company as 0.018  
332 cm<sup>2</sup>. Fig. 2B shows the  $Sf$  stationary phase retention volume ratio plotted versus the  
333 corresponding mobile phase velocity  $u$ .

334 The interesting result evidenced by Fig. 2B is that at moderate centrifugal force (<400  $g$ )  
335 there is clearly a maximum possible mobile phase velocity explaining the slope changes seen  
336 in Fig. 2A. Fig. 2B shows that at 112  $g$  (1000 rpm), the mobile phase velocity cannot exceed 9  
337 m/min (closed arrow in Fig. 2B) reached at 7 mL/min. At 1000 rpm and above 7 mL/min,

338 any flow rate increase is exactly compensated by a  $Sf$  reduction in term of velocity (eq. 6).  
339 Similarly, a maximum velocity,  $u = 11$  m/min (open arrow in Fig. 2B), is observed with the  
340 365  $g$  centrifugal force at 1800 rpm. This trend seems to be valid for higher centrifugal forces  
341 since a maximum velocity of 13 m/min (blue arrow in Fig. 2B) is observed at 545  $g$  (2200  
342 rpm). It becomes difficult to make observation at higher centrifugal forces since the  
343 theoretical linear line of  $Sf$  versus  $F$  transposes with the 30-mL rotor in a maximum velocity  $u$   
344 of 15 m/min (dotted lines in Fig. 2) for which there is no stationary phase left in the rotor ( $Sf$   
345 = 0). Higher flow rates are technically possible, but this is no longer chromatography since  
346 there is no stationary phase to interact with the moving phase. A direct linear relationship  
347 between this observed maximum velocity and rotor rotation seems to exist as shown by the  
348 inset in Fig. 2B.

349

350

### 351 3.2 Driving pressure

352 The  $Sf$  study shows that the maximum centrifugal force will give the highest stationary  
353 phase retention at high flow rates needed to obtain fast separations. However CPC  
354 instruments use rotary seals with strict pressure limitation. A rotary seal is a mechanical  
355 component with a flat flanged stator, a fixed part, on which a rotating piece with flat flange  
356 fitting the stator is pressed allowing to connect a rotating tube to a motionless one. If  
357 different designs exist, rotary seals have all two inherent problems: i) the rotating part in  
358 contact with the static part generates heat, ii) above a certain pressure, the liquid inside the  
359 rotary seal can percolate between the mobile and static parts. This phenomenon is reversible,  
360 but when solvents leak in a rotary seal, they dissolve the lubricants of the ball-bearings  
361 damaging them. The rotary seals of our CPC frame could withstand pressure up to 70 bars.  
362 The working pressure was noted for all experiments and the pressure safety switch was set at  
363 70 bars stopping automatically the pump if this limit was passed.

364

365 The experimental pressure was read when the 30-mL rotor was equilibrated at different  
366 flow rates and rotor rotation speeds. It was proposed that  $\Delta P$ , the CPC column driving  
367 pressure, could be expressed as:

368

$$369 \quad \Delta P = a.Sf.\Delta\rho.\omega^2 + b.\eta.F \quad \text{eq. 7}$$

370

371 in which  $\Delta\rho$  is the density difference (g/mL) between the mobile and stationary liquid  
372 phases,  $\omega^2$  is the rotor angular velocity (rd<sup>2</sup>/s<sup>2</sup>),  $\eta$  is the mobile phase viscosity (cP or Pa.s)  
373 and  $a$  and  $b$  are rotor related geometrical constants [1, 2, 19, 22]. The first term of Eq. 7 is the  
374 hydrostatic term where pressure is generated by the centrifugal force and the two liquid  
375 phases present in the rotor cells. The second term is the pressure contribution due to the  
376 mobile phase viscosity (Darcy law). If the hydrostatic term depends on both centrifugal force  
377 and flow since  $Sf$  is flow related, the hydrodynamic second term depends on flow only.

378 From a driving pressure point of view, low mobile phase flow rates ( $F < 5$  mL/min and  
379 high  $Sf$  values, Fig. 2) are not possible at fast rotor rotations: the driving pressure would pass  
380 the 70 bar rotary seal requirement. This is not a problem since low mobile phase flow rates  
381 are associated with high experiment durations and low productivity. As far as pressure is

382 concerned, high mobile phase flow rates are possible at all rotor rotation speeds of our  
383 apparatus (1000-3000 rpm). The hydrodynamic viscous pressure in our experimental  
384 conditions (30-mL rotor and aqueous lower phase of the HEMWat O or AZ N system) would  
385 reach 70 bars at a flow rate of 57 mL/min. No practical experiments are possible at this high  
386 flow rate since there would be no stationary phase left in the 30-mL column (Fig. 2). At 20  
387 mL/min, there is about 20% of stationary phase still remaining in the 30-mL rotor for  
388 rotation higher than 2000 rpm (Fig. 2A) and the driving pressure stays within 40-60 bars  
389 below the maximum rotary seal limit. At 20 mL/min, the 33.2 mL column volume is swept in  
390 1.6 min, a very reasonable time allowing for fast separations.

391

392

### 393 3.3 Chromatographic efficiency

394 Eq. 3 shows that the chromatographic efficiency  $N$ , expressed in theoretical plate number,  
395 is related to peak width. A higher efficiency produces thinner peaks increasing resolution  
396 and/or allowing higher loads in preparative purifications. Table 3 lists the full data obtained  
397 with the Fig. 1 separation examples.

398 In liquid chromatography with a solid stationary phase, i.e. LC techniques,  $H$ , the height  
399 equivalent to a theoretical plate or plate height, reflects the chromatographic variance per  
400 unit length, allowing comparing efficiencies between columns of different geometries (length,  
401 diameter, particle size). Plots of  $H$  versus mobile phase velocity, generally referred to as van  
402 Deemter plots, are undoubtedly the most popular graphical representation of LC  
403 chromatographic performance. The plot is based on the assumption that the plate height is  
404 independent of the column length. Under similar assumption, in CPC, the number of cells  
405 equivalent to a theoretical plate,  $NC/TP$ , can be used noting that a lower  $NC/TP$  value is  
406 better.

407 Fig. 3 shows the rotor efficiency plotted as the number of cells equivalent to a theoretical  
408 plate  $NC/TP$ , for the two retained peaks: coumarin ( $K = 1.3$ ) and carvone ( $K = 7.3$ ) versus the  
409 mobile phase linear velocity  $u$  (Figs. 3 A and B) and versus  $Sf$  the stationary phase retention  
410 volume ratio in the 30-mL rotor (Figs. 3C and D).

411 The clear trend shows by Fig. 3A and 3B is a significant increase in efficiency when the  
412 applied centrifugal force (rotor rotation) increases. For example, at 10 m/min and 365  $g$  (11  
413 mL/min and 1800 rpm), the  $NC/TP$ s are 1.9 and 3.5 for coumarin and carvone, respectively,  
414 corresponding to 438 and 237 plates in the 30-mL rotor (832 cells). Working at lower  
415 centrifugal force (112  $g$ , 1000 rpm) has dramatic consequences, with more than 8 cells  
416 required to make one plate. A high centrifugal field is highly beneficial to the  
417 chromatographic efficiency. At 10 m/min and 882  $g$  (2800 rpm), the  $NC/TP$  is as low as 0.8  
418 for both coumarin and carvone (corresponding to 1080 plates), demonstrating that every  
419 single cell is indeed active in the efficient mixing and resulting chromatographic exchange.  
420 Here we assume a uniform distribution of the two liquid phases throughout the CPC rotor. A  
421 reviewer pointed out that the first cells at the rotor entrance may contain less stationary  
422 phase (higher pressure) than the last cells at the rotor end (low pressure). We have no mean  
423 to check this possible dynamic state and present the average values read on the experimental  
424 chromatograms.

425 Figs 3A and B show the number of cells equivalent to one theoretical plate plotted versus  
426 mobile phase velocity for the solute with low chromatographic retention (coumarin,  $K = 1.3$ ,

427 Fig. 3A) and the one highly retained (carvone,  $K = 7.3$ , Fig. 3B). These plots exhibit specific  
428 shapes that are typical from chromatographic dispersions. At low mobile phase velocity,  
429 solutes are submitted to molecular diffusion both in mobile and stationary phase and the  
430 NC/TP varies as  $\frac{1}{u}$ . At high mobile phase velocity, solute dispersion is mainly driven by  
431 mass transfer and highly retained compounds exhibit large band broadening (NC/TP = 4.8  
432 for carvone at 1800 rpm, 11 m/min) while for compounds with  $K$  close to 1, the linear velocity  
433 has very little influence on the NC/TP (being 2 for coumarin at 1800 rpm, 11 m/min). These  
434 observations are very close to solute behavior in LC process (Van Deemter curves).  
435 Increasing the applied centrifugal field reduces both diffusion and mass transfer  
436 contributions to chromatographic dispersions, reaching the optimal performances of 1 cell  
437 per theoretical plate at 2500 rpm for the less retained coumarin compound and at 2800 rpm  
438 for the more retained carvone compound.

439 As a consequence, it is confirmed that the best efficiencies are obtained at high rotational  
440 speed and elevated linear velocity [1, 7, 8, 19]. But it is crucial to remember that, in CPC,  
441 rotation speed is constraint by pressure, while a maximum mobile phase linear velocity  
442 cannot be exceeded. Increasing the flow rate results in increasing the linear velocity up to its  
443 maximal value, but then all further flow rate increases will only reduce the working liquid  
444 stationary phase volume ratio,  $Sf$ , being deleterious for the purification.

445 Fig. 3C and 3D show the same efficiencies expressed as NC/TP plotted versus the  $Sf$   
446 values. The increase in efficiency as the centrifugal force increases is obviously confirmed.  
447 However, a decrease in efficiency is associated with more stationary phase in the rotor. This  
448 decrease is severe at high centrifugal forces with the less retained coumarin compound (Fig.  
449 3C). For example, at 882  $g$  (2800 rpm), the coumarin NC/TP is 0.7 (1200 plates) at  $Sf =$   
450 25%, reaching NC/TP = 1.25 (666 plates) at  $Sf = 33\%$ . This efficiency reduction with  
451 increased  $Sf$  is less severe for the more retained carvone compound (Fig. 3D) and for lower  
452 centrifugal forces. With this 30-mL rotor, working at maximal  $Sf$  is detrimental to efficiency.

453 Since the resolution factor is defined as the distance between peak apexes divided by the  
454 average peak widths (Eq. 5), it is maximized when stationary phase retention volume ratio,  
455  $Sf$ , is large and peak broadening is low. Thus, for low retained compounds, centrifugal forces  
456 of 2500 rpm will provide as good a resolution as 2800 rpm, while for highly retained  
457 compounds, the increase of centrifugal force will be highly beneficial on resolution factor.

458 While resolution is best at low flow rate due to the large contribution of  $Sf$ , it results in  
459 long analysis times. However, if the selectivity factor ( $K_2/K_1$  ratio) is large enough, it is worth  
460 working at higher flow rates to speed up the separations: the gain in higher throughput  
461 compensates for the loss of resolution associated with the reduced  $Sf$  (Fig. 2). The efficiency  
462 being higher at reduced  $Sf$  and high flow rates, thinner peaks should allow for increased rotor  
463 loads provided the space between peaks remains acceptable [24].

464

465

### 466 3.4 Free space between peak and throughput estimation

467 In a recent work, we proposed to use the free space between two adjacent peaks as a  
468 convenient estimate of the loading capability in a large scale rotor using the results obtained  
469 in a small CPC rotor [24]. The free space between peaks  $\Delta V$  is related to the retention  
470 difference between the two peaks; that is the numerator of the resolution equation (Eq. 5).

471 Since the Gaussian peak base is equal to  $4\sigma$ , the free space between peaks cumulates the  
472 retention difference and the peak dispersions that are related to the denominator of the  
473 resolution equation and to efficiency (Eqs. 5 and 1).

474 Fig. 4A shows the experimental  $\Delta V$  volume between the coumarin and carvone peaks  
475 measured in all operating conditions with the 30-mL rotor and HEMWat o (AZ N) system.  
476 The trend is an increased space between peaks when more stationary phase is in the rotor.  
477 This trend is expected since the  $\Delta V$  difference is directly related to  $V_S$ . However, since  $Sf$   
478 decreases with increasing flow rates (Fig. 2), it seems that it will not be possible to work with  
479 a good productivity at high flow rates. The time needed to complete the separation is a factor  
480 that must be taken in account.

481 Fig. 4B shows the evolution of a productivity factor defined as  $\Delta V/t'_R$ , with  $t'_R$  being the  
482 carvone retention time (peak crest) plus two  $\sigma$  (Eq. 1) corresponding to the delay needed to  
483 return to baseline. The  $\Delta V/t'_R$  parameter gives a good idea of the throughput that will be  
484 possible to get in performing repetitive purification loads [24]. If the study confirms that a  
485 high centrifugal force (high rotor rotation) is needed to obtain a significant productivity, it  
486 shows that the maximum rotor rotation and maximum flow rate may not be necessarily the  
487 most appropriate settings to obtain the highest productivity with this particular 30-mL rotor.  
488 An optimum flow rate between 15 and 18 mL will give the highest productivity. We note that  
489 this optimum flow rate corresponds to the lowest flow rate giving the maximum mobile phase  
490 velocity observed in Section 3.1 and Fig. 2B. Higher flow rates deplete so much the stationary  
491 phase that the peaks cannot be enough separated. The existence of an optimal flow rate for  
492 the highest productivity was already highlighted in our previous work for GUESS compounds  
493 separation using HEMWat solvent systems on 30-mL and 259-mL rotors [24] and more  
494 recently on the 259-mL rotor for rosemary extract separation using heptane/MtBE/  
495 ethanol/water 4:1:4:1 v/v [25].

496 Also, in the conditions of this study, the 8% productivity gain between the highest 2800  
497 rpm rotation at 18 mL/min (open squares in Fig. 4B) and the 2200 rpm rotation at 16  
498 mL/min (triangles in Fig. 4B) may not be worth the trouble and cost of more rapid rotary seal  
499 wearing.

500

501

### 502 3.5 Working with the 80-mL rotor

503 The 80-mL rotor was engineered for preparative purification at high flow rate. Compared  
504 with the 30-mL rotor, it is made with twice less cells that are almost five times bigger (Table  
505 1) with a larger "bore" (average rotor cross section of  $3.1 \text{ mm}^2$ ) for easier liquid flowing.  
506 Considering the dedicated use of this rotor, it was studied at flow rates higher than 10  
507 mL/min and rotor rotations of 2200 rpm, 2500 rpm and 2800 rpm, i.e. high centrifugal  
508 forces of 545, 712 and 882 g (Table 2).

509

#### 510 *Stationary phase retention*

511 Fig. 5A and 5B should be compared with Fig. 2A and 2B. The linear decrease of  $Sf$  is  
512 observed up to a flow rate of 33 mL/min above which the 80-mL rotor retains more liquid  
513 stationary phase than expected (Fig. 5A). This experimental result let us think that the cell  
514 design may allow for a small part of liquid stationary phase to be trapped and not swept by

515 the mobile phase at high flow rates. The consequence is that there is no maximum linear  
516 velocity as observed with the 30-mL rotor. Fig. 5B shows that the mobile phase linear  
517 velocity keep increasing with the flow rate up to the maximum 55 mL/min tested,  
518 corresponding to a mobile phase velocity of 22 m/min. Higher linear velocities seem  
519 possible.

520

#### 521 *Driving pressure*

522 The driving pressures obtained in the two rotors were compared. The trend is the same:  
523 high flow rates do not produce higher driving pressure as long as there is some liquid  
524 stationary phase remaining in the rotor. The design of the 80-mL rotor with less cells of  
525 larger volume and connecting ducts with larger bore allows running the 80-mL rotor at flow  
526 rates three times higher than what was permitted with the smaller 30-mL rotor. Our  
527 experimental set-up was limited to a maximum flow rate of 60 mL/min. Much higher flow  
528 rates could be envisaged with the 80-mL rotor assuming 10-12% of liquid stationary phase  
529 stay trapped in it. The hydrodynamic pressure would be the limiting factor. At 55 mL/min  
530 and 2800 rpm, the experimental driving pressure is 31 bar well below the maximum 70 bar of  
531 the rotary seals. The observed 31 bar are made of 11 bar hydrostatic pressure (35%, Eq. 7)  
532 and 20 bars (65%) hydrodynamic pressure. Assuming that 10% of stationary phase stay  
533 trapped in the 80-mL rotor ( $Sf = 10\%$ ), Eq. 7 allows to estimate the limiting flow rate to be  
534 170 mL/min generating 62 bars of hydrodynamic pressure with only 8 bars due to the  
535 hydrostatic contribution at 2800 rpm.

536

#### 537 *Efficiency*

538 Because of the lower number of cells (406 cells), the plate number is at least two times  
539 lower with the 80-mL rotor. In order to compare instruments performances, the number of  
540 cells equivalent to one theoretical plate (NC/TP) was plotted versus mobile phase linear  
541 velocity,  $u$ , for the 80-mL rotor (Fig. 6, to be compared to Fig. 3). The dispersion is driven by  
542 diffusion at low velocity, as mainly illustrated by the coumarin behavior, while the  
543 contribution to mass transfer is no longer visible, as expected by the supplier for this new  
544 design.

545 For compounds with low retention such as coumarin, the small rotor performs slightly  
546 better than the 80-mL rotor when working at identical velocity. At 11 m/min and 2800 rpm,  
547 the 30-mL rotor requires only 0.6 cells to make one theoretical plate (Fig. 3A), while the 80-  
548 mL rotor requires 1.0 cell in the same operating conditions (Fig. 6A). However, the 80-mL  
549 rotor is designed to work faster and its performances reach 0.6 NC/TP at 20 m/min. It  
550 means that if this new design had 832 cells, it could provide the same number of plates as the  
551 30-mL commercial rotor (1390 plates) while working at 50 mL/min.

552 While the highly retained carvone NC/TP was  $g$ -field dependent with the small 30-mL  
553 rotor (in the range 0.8-2.7, Fig. 3B), the 80-mL rotor provides an efficient mixing and mass  
554 transfer for all tested centrifugal forces with carvone NC/TP in the narrow 1.5-2.0 range.

555 When relating the experimental efficiencies to  $Sf$ , the ratio of stationary phase volume  
556 retained by the column, the trend of Fig. 3C and 3D was also observed with the 80-mL rotor.  
557 Coumarin shows a regular efficiency decrease when  $Sf$  increases. This trend is less important  
558 for carvone whose efficiency changes were more limited.

559

#### 560 *Peak space between peaks and throughput estimation*

561 For the 30-mL rotor, Fig. 4A shows a  $\Delta V$  space between carvone and coumarin peak  
562 increasing between 20 and 120 mL as  $Sf$  increases for 10 to 70%. The picture with the 80-mL  
563 rotor is similar with a  $\Delta V$  space between peak increasing between 80 mL for  $Sf = 15\%$  going  
564 as high as 200 mL for  $Sf = 60\%$ . This is illustrated by Fig. 1 showing a chromatogram done at  
565 the same 2500 rpm on the two rotors. The efficiencies obtained with the 80-mL rotor are  
566 lower meaning broader peaks in the time space shown by the figure. However, the flow rate  
567 in the 80-mL rotor being much higher (45 mL/min) compared to the 11 mL/min in the 30-  
568 mL rotor, the  $\Delta V$  space between coumarin and carvone is 88 mL with the 80-mL rotor almost  
569 twice the 49 mL of the 30-mL rotor (Table 3).

570 When throughput is considered introducing the time needed to complete the separation,  
571 the higher flow rates possible with the 80-mL rotor clearly shows the interest of this rotor for  
572 preparative purification. The  $\Delta V/t'_R$  parameter obtained with the 10-55 mL/min data of the  
573 80-mL rotor shows a regular increase with the flow rate,  $F$ . However, no maximum values as  
574 seen in Fig. 4B were obtained. The maximum theoretical productivity was seen at 17 mL/min  
575 with a  $\Delta V/t'_R$  value of 6.5 mL/min for the 30-mL rotor (Fig. 4B). For the 80-mL rotor, the  
576 highest theoretical productivity was obtained at the maximum flow rate tested, 55 mL/min,  
577 with a  $\Delta V/t'_R$  value of 18 mL/min. Higher flow rates are possible and would give better  
578 productivity. The three  $\Delta V/t'_R$  versus  $F$  lines obtained with the three rotor rotations tested  
579 were similar. This indicates that, in our particular experimental conditions, it is best to work  
580 at 2200 rpm reducing strain and wearing of the equipment, still obtaining the best  
581 productivity.

582

583

#### 584 **4. Conclusion**

585

586 Using a simple separation of test solutes and working only at analytical concentrations  
587 with a small 30-mL rotor and a larger 80-mL rotor of different configuration, a large set of  
588 operating conditions was tested with the heptane/ethyl acetate/methanol/water 1:1:1:1 v/v  
589 HEMWat zero or Arizona N system. It is confirmed that the amount of liquid stationary  
590 phase retained in the rotor decreases linearly when the flow rate of the mobile phase  
591 increases. In our experimental conditions, a maximum linear velocity of the mobile phase  
592 was observed with the 30-mL rotor: in a given centrifugal force (rotor speed), the mobile  
593 phase cannot pass a maximum linear velocity. When this maximum velocity is reached,  
594 increasing the flow rate will just deplete the stationary phase so that the linear mobile phase  
595 velocity stays the same, up to a complete washing of all stationary phase off the rotor.

596 The 80-mL rotor exhibits the same stationary phase retention decreasing linearly with  
597 flow rate increases. However, this trend was somehow stopped above 35 mL/min, where it  
598 was observed that the mobile phase flow could not expel 10 to 15% of the stationary phase  
599 contained in the rotor making separations possible at very high flows.

600 The study of the experimental chromatographic efficiency was performed using the  
601 concept of NC/TP: number of cells needed to make one theoretical plate, as representative of  
602 peak width. It is confirmed with the two rotors that a higher centrifugal force (higher rotor

603 rotation) and higher flow rates produced sharper peaks (more plates). However, when  
604 preparative purifications are the goal of the CPC separation, it was shown that an optimum  
605 flow rate for best throughput existed with the 30-mL rotor. This optimum could not be  
606 reached with the 80-mL rotor due to hardware limitation.

607 This attempt of generic column characterization should of course be taken with care as it  
608 is solvent system- and rotor design-dependent. From a user's perspective, the sample to  
609 purify should be considered. Selecting a liquid system in which the compound to purify is  
610 well separated from impurities, being significantly retain (e.g.  $K > 5$ ), it may be of interest to  
611 work at high flow rate with an optimized amount of stationary phase. A prejudice would be  
612 to think that working at the highest stationary phase retention (i.e. the highest rotor rotation)  
613 provides the best results. On the contrary, it often leads to unnecessary long separations and  
614 broad peaks, damaging the reputation of the CPC technique.

615

616

## 617 **Acknowledgements**

618 AB and KF thanks the French Centre National de la Recherche Scientifique for  
619 continuous support through ISA-UMR 5280. KF thanks the Rousselet-Robatel Kromaton  
620 company for the loan of the 80-mL rotor prototype.

621

622

## 623 **References**

624

- 625 [1] A.P. Foucault, Centrifugal Partition Chromatography, Chromatogr. Sci. Ser., vol. 68, M.  
626 Dekker, New York, 1992.
- 627 [2] A. Berthod, Countercurrent chromatography: the support-free liquid stationary phase,  
628 Comprehensive Analytical Chemistry, vol. 38, Elsevier, 2002.
- 629 [3] Y. Ito, W.D. Conway, High-Speed Countercurrent Chromatography, Chemical Analysis,  
630 J. Wiley, 1996.
- 631 [4] K. Skalicka-Wozniak, I. Garrard, A comprehensive classification of solvent systems used  
632 for natural product purifications in countercurrent and centrifugal partition  
633 chromatography, Nat. Prod. Rep., 32 (2015) 1556-1561.
- 634 [5] Y. Liu, J.B. Friesen, J.B. McAlpine, G.F. Pauli, Solvent system selection strategies in  
635 countercurrent separation, Planta Medica, 81 (2015) 1582-1591.
- 636 [6] Y. Ito, Golden rules and pitfalls in selecting optimum conditions for high-speed  
637 counter-current chromatography, J. Chromatogr. A, 1065 (2005) 145-168.
- 638 [7] L. Marchal, A. Foucault, G. Patissier, J.M. Rosant, J. Legrand, Influence of flow  
639 patterns on chromatographic efficiency in centrifugal partition chromatography, J.  
640 Chromatogr. A, 869 (2000) 339-352.
- 641 [8] L. Marchal, J. Legrand, A. Foucault, Mass transport and flow regimes in centrifugal  
642 partition chromatography, AIChE J. 48 (2002) 1692-1704.
- 643 [9] S. Chollet, L. Marchal, J. Meucci, J.H. Renault, J. Legrand, A. Foucault, Methodology  
644 for optimally sized centrifugal partition chromatography columns, J. Chromatogr. A,  
645 1388 (2015) 174-183.

- 646 [10] S. Adelman, C. Schwienheer, G. Schembecker, Multiphase flow modeling in  
647 centrifugal partition chromatography, *J. Chromatogr. A*, 1218 (2011) 6092-6101.
- 648 [11] S. Adelman, G. Schembecker, Influence of physical properties and operating  
649 parameters on hydrodynamics in centrifugal partition chromatography, *J. Chromatogr.*  
650 *A*, 1218 (2011) 5401-5413.
- 651 [12] C. Schwienheer, J. Merz, G. Schembecker, Investigation, comparison and design of  
652 chambers used in centrifugal partition chromatography on the basis of flow pattern and  
653 separation experiments, *J. Chromatogr. A*, 1390 (2015) 39-49.
- 654 [13] A. Berthod, M. Hassoun, M.J. Ruiz-Angel, Alkane effect in the Arizona liquid systems  
655 used in countercurrent chromatography, *Anal. Bioanal. Chem.*, 383 (2005) 327-340.
- 656 [14] J.B. Friesen, G.F. Pauli, GUESS – A generally useful estimate of solvent system in CCC,  
657 *J. Liq. Chromatogr. Rel. Technol*, 28 (2005) 2777-2806.
- 658 [15] J.B. Friesen, G.F. Pauli, Rational development of solvent system families in CCC, *J.*  
659 *Chromatogr. A*, 1151 (2007) 51-59.
- 660 [16] P.L. Wood, D. Hawes, L. Janaway, I.A. Sutherland, Stationary phase retention in CCC:  
661 modeling the J-type centrifuge as a constant pressure drop pump, *J. Liq. Chromatogr.*  
662 *Rel. Technol.* 26 (2003) 1373-1396.
- 663 [17] A. Berthod, K. Faure, Revisiting resolution in hydrodynamic countercurrent  
664 chromatographic: tubing bore effect, *J. Chromatogr. A*, 1390 (2015) 71-77.
- 665 [18] A.P. Foucault, O. Bousquet, F. Le Goffic, J. Cazes, Countercurrent chromatography with  
666 a new centrifugal partition chromatographic system, *J. Liq. Chromatogr.* 15 (1992)  
667 2721-2733.
- 668 [19] A. P. Foucault, Theory of centrifugal partition chromatography, in *Centrifugal Partition*  
669 *Chromatography*, A.P. Foucault, ed., *Chromatogr. Sci. Ser.*, Vol. 68, Ch. 2, 25-49, 1992.
- 670 [20] A. Kotland, S. Chollet, J.M. Autret, C. Diard, L. Marchal, J.H. Renault, Modeling pH-  
671 zone refining CCC: a dynamic approach, *J. Chromatogr. A*, 1391 (2015) 80-87.
- 672 [21] S. Adelman, T. Baldhoff, B. Koepcke, G. Schembecker, Selection of operating  
673 parameters on the basis of hydrodynamics in centrifugal partition chromatography for  
674 the purification of nybomycin derivatives, *J. Chromatogr. A* 1274 (2013) 54-64.
- 675 [22] D.W. Armstrong, G.L. Bertrand, A. Berthod, Study of the origin and mechanism of band  
676 broadening and pressure drop in centrifugal countercurrent chromatography, *Anal.*  
677 *Chem.* 60 (1988) 2513-2519.
- 678 [23] L. Marchal, O. Intes, A.P. Foucault, J. Legrand, J.M. Nuzillard, J.H. Renault, Rational  
679 improvement in CPC settings for the production of 5-*n*-alkylresorcinols from wheat  
680 bran lipid extract: I. Flooding conditions-optimizing the injection step, *J. Chromatogr.*  
681 *A* 1005 (2003) 51-62.
- 682 [24] E. Bouju, A. Berthod, K. Faure, Scale-up in CPC: the "free-space between peaks"  
683 method, *J. Chromatogr. A* 1409 (2015) 70-78.
- 684 [25] E. Bouju, A. Berthod, K. Faure, Carnosol purification. Scaling-up centrifugal partition  
685 chromatography separations, *J. Chromatogr. A* in press  
686 <http://dx.doi.org/10.1016/j.chroma.2016.08.015> 2016.
- 687

688  
689  
690  
691  
692  
693  
694

**Table 1:** Characteristics of the two tested CPC rotors.

<b>Rotor denomination</b>	Measured volume mL	Cell number	Cell shape	Cell volume $\mu\text{L}$	Total duct volume mL	Maximum $Sf^*$	Total cell volume mL
<b>30-mL</b>	33.25	832	Twin <b>8</b> shaped	30	8.3	74.9%	24.9
<b>80-mL</b>	83.4	406	Twin proprietary	144	25.0	70.0%	58.4

695  
696  
697  
698  
699  
700  
701  
702  
703  
704  
705

\*Twin-cells are interconnected by duct canals that can contain mobile phase only, hence there is a maximum theoretical  $Sf$  corresponding to all twin-cells filled by stationary phase.

**Table 2:** Centrifugal fields generated by different rotation speeds for the two CPC rotors with an average 10-cm distance of the cells from the axis of rotation.

<b>Rotation speed (rpm)</b>	1000	1800	2200	2500	2800
<b>Angular velocity (<math>\omega</math>, rd/s)</b>	105	188	230	262	293
<b>Centrifugal field (<math>g^a</math>)</b>	112	365	545	712	882

706  
707

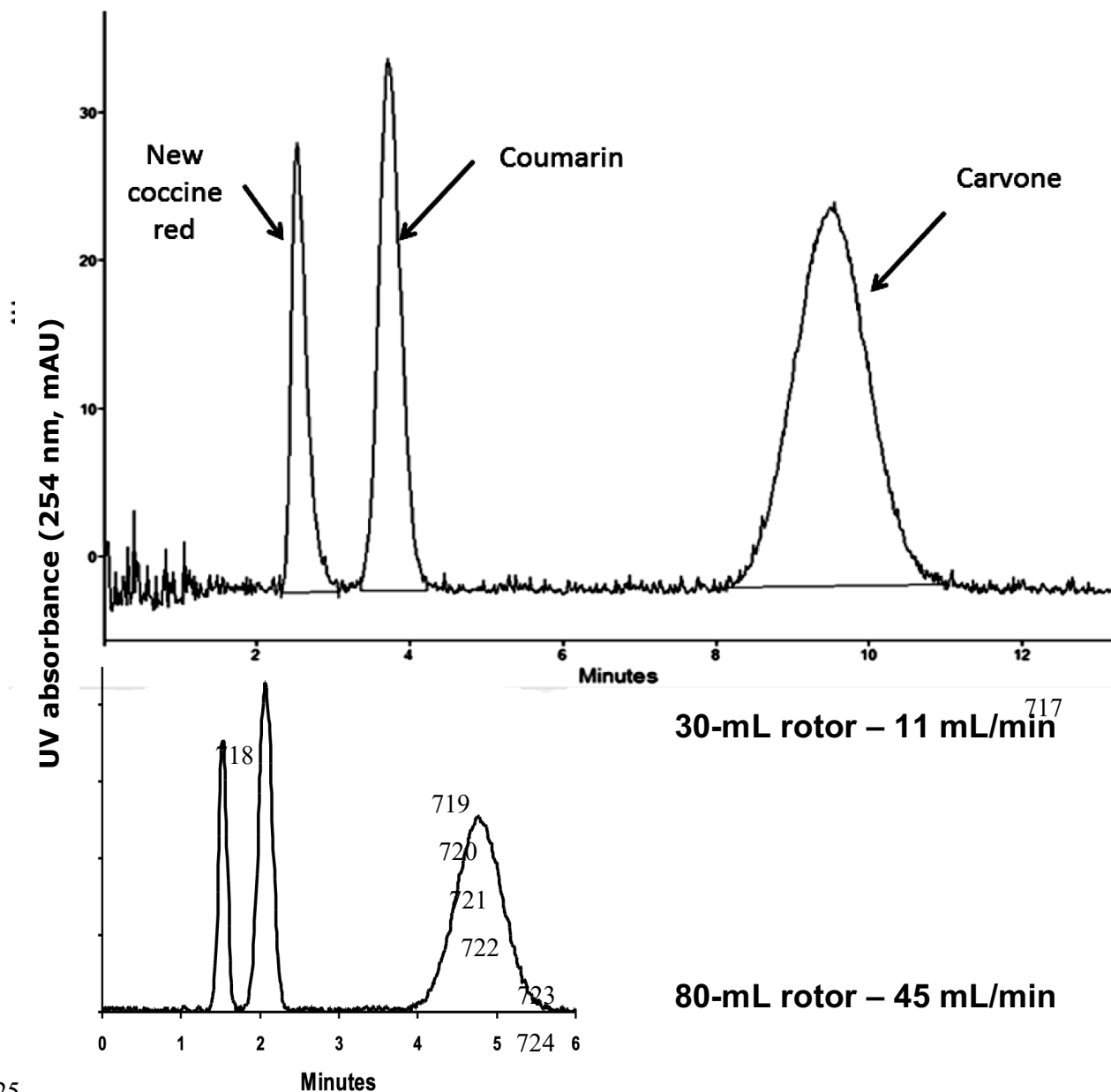
a)  $g$  is the earth average gravitational field equal to  $9.81 \text{ m/s}^2$

708  
709  
710  
711  
712  
713

**Table 3 :** Data corresponding to the Fig. 1 chromatogram.

Parameter / Compounds	New coccine red	Coumarin	Carvone
<b>Rotor 30-mL</b>			
t <sub>R</sub> (min)	2.52	3.70	9.53
V <sub>R</sub> (mL)	27.7	40.7	104.8
Calculated K	0	1.25	7.41
Peak width at 1/2 h (mL)	2.2	3.6	11.5
N observed (plates)	900	720	460
N effective (plates)	-	1030	480
Cells for one theoretical plate		0.8	1.7
ΔV (mL)	7	49	
ΔV/t' (mL/min)	1.8	4.8	
<b>Rotor 80-mL</b>			
t <sub>R</sub> (min)	1.53	2.07	4.78
V <sub>R</sub> (mL)	68.9	93.1	215
Calculated K	0	1.24	7.49
Peak width at 1/2 h (mL)	5.7	8.9	30.9
N observed (plates)	800	610	270
N effective (plates)		680	275
Cells for one theoretical plate		0.6	1.5
ΔV (mL)	9.5	88	
ΔV/t' (mL/min)	4.3	16.5	
<b>CPC conditions and rotor data</b>		<b>30 mL</b>	<b>80 mL</b>
30-mL top chromatogram 80-mL bottom chromatogram	Rotation (rpm) Centrifugal force	2500 712 g	2500 712 g
	Flow rate (mL/min)	11	45
	V <sub>C</sub> (mL)	33.2	83.4
	Average cross section (mm <sup>2</sup> )	1.8	3.1
	Extra-column volume (mL)	4.9	4.9
	V <sub>M</sub> (mL)	27.7	68.9
	V <sub>S</sub> (mL)	10.4	19.5
	Sf	31.3%	23.4%
	Linear velocity (m/min)	9	19.5
Pressure (bar)	51	32	

714  
715  
716



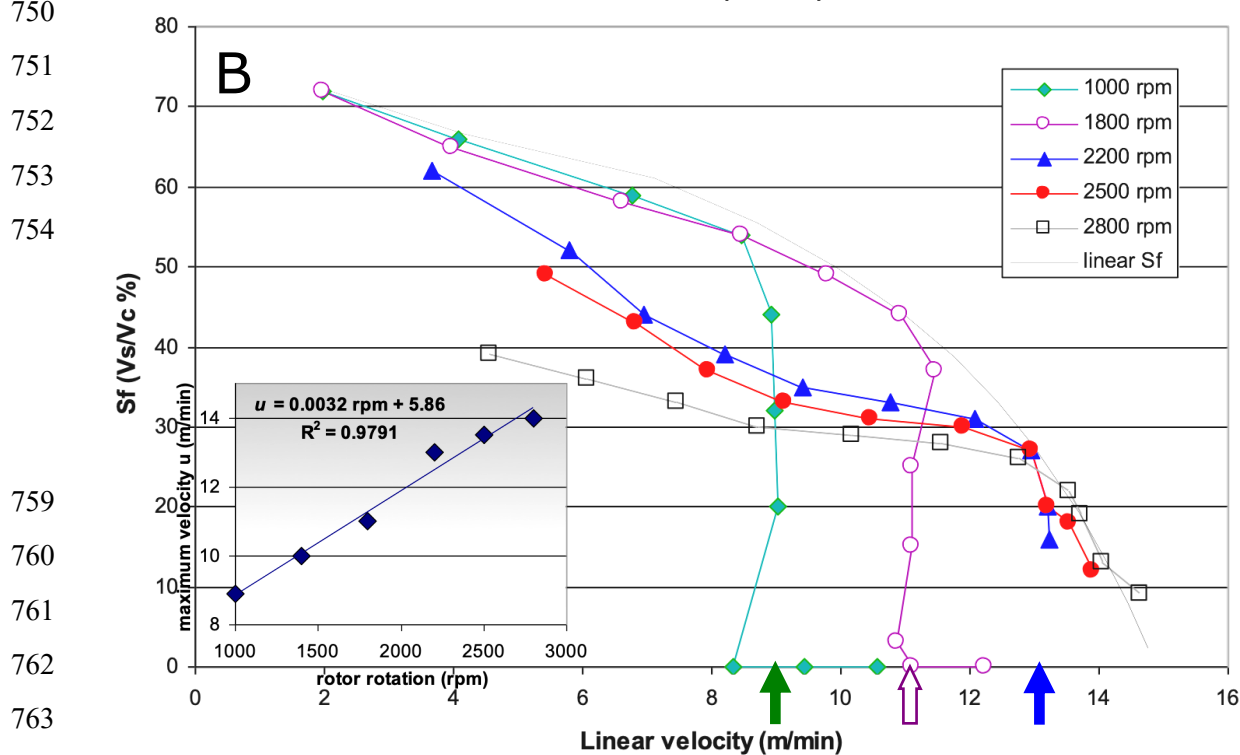
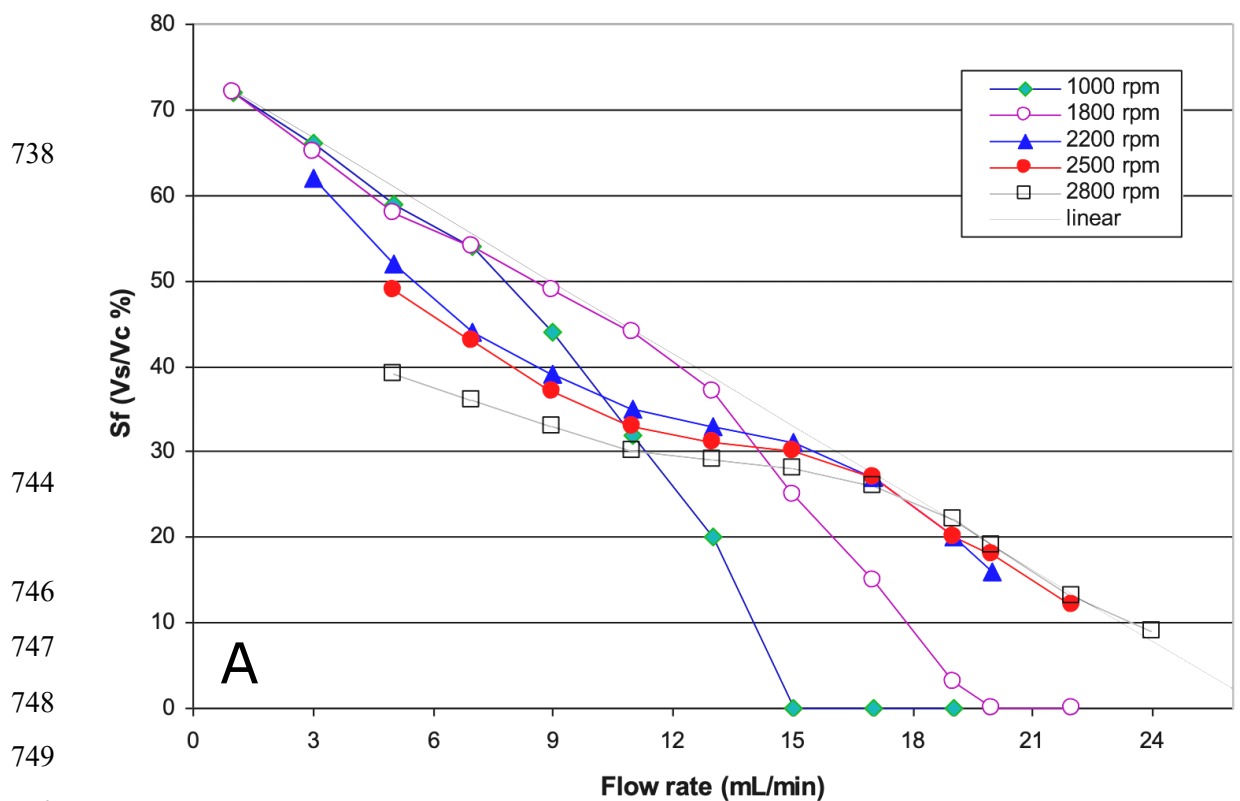
725

726

727 **Figure 1.** Chromatograms of new coccine red (0.25 mg), coumarin (0.75 mg) and carvone  
 728 (1.25 mg) separated with the liquid system HEMWat O (Arizona N): heptane/ethyl  
 729 acetate/methanol/water 1:1:1:1 v/v, descending mode. Injection volume 0.5 mL. Top:  
 730 column 30-mL rotor, flow rate: 11 mL/min, 712 g (2500 rpm),  $V_M = 27.7$  mL, stationary  
 731 phase retention (volume ratio)  $S_f = 31.3\%$ , 51 bar, UV 254 nm. Bottom: column 80-mL, flow  
 732 rate: 45 mL/min, 712 g (2500 rpm),  $V_M = 68.8$  mL, stationary phase retention volume ratio  
 733  $S_f = 23.4\%$ , 32 bar, UV 254 nm. See Table 3 for full experimental details.

734

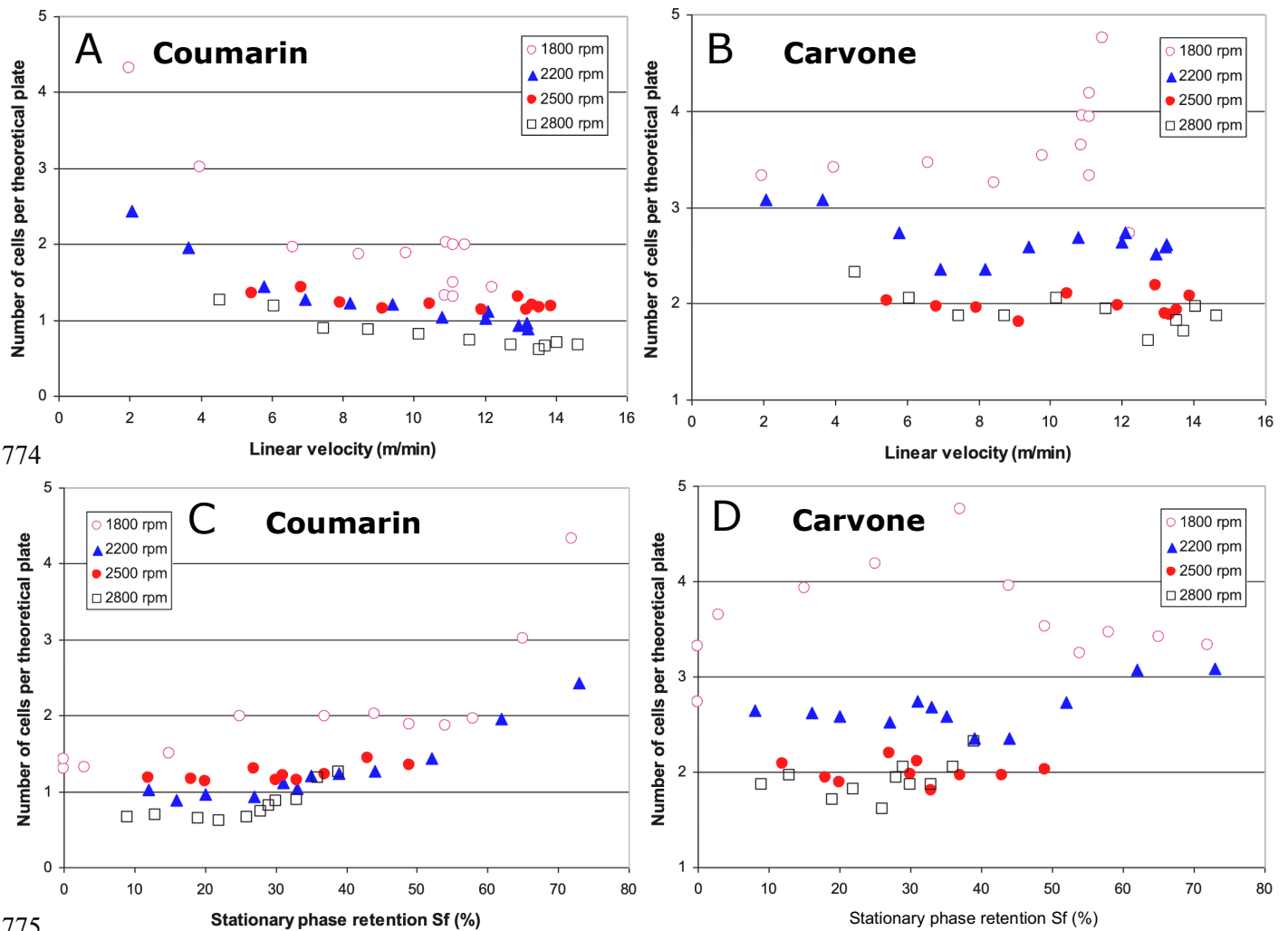
735



765 **Figure 2.** Organic upper stationary phase retention (volume ratio),  $S_f$ , versus **A**-the  
 766 aqueous mobile phase flow rate (mL/min) and **B**-the aqueous mobile phase velocity (m/min)  
 767 at different 30-mL rotor rotations. The dotted lines correspond to the linear relation:  $S_f =$   
 768  $75\% - 2.8 F$  (2A) transposed by eq. 4 in 2B. The arrows point at maximum velocities. The  
 769 lower left inset shows the maximum velocities plotted versus rotor rotation.

770

771  
772  
773



774

775

776

777 **Figure 3.** Coumarin (left) and carvone (right) peak experimental efficiency expressed as  
778 the number of cells needed for one theoretical plate (NC/TP, lower is better) plotted versus  
779 the mobile phase linear velocity (top figures A and B) and Sf, the volume ratio of stationary  
780 phase retained in a 30-mL CPC rotor (bottom figures C and D) spinning at indicated rotation  
781 speeds. Rotor of 832 twin-cells. System HEMWat o (AZ N) heptane/ethyl  
782 acetate/methanol/water 1:1:1:1 v/v, aqueous lower phase in the descending mode.

783

784  
785  
786  
787  
788  
792  
793  
794  
795  
796  
797  
798  
799  
800  
801  
802  
803  
804  
805  
806  
807  
808  
809  
810  
811  
812  
813  
814  
815  
816  
817

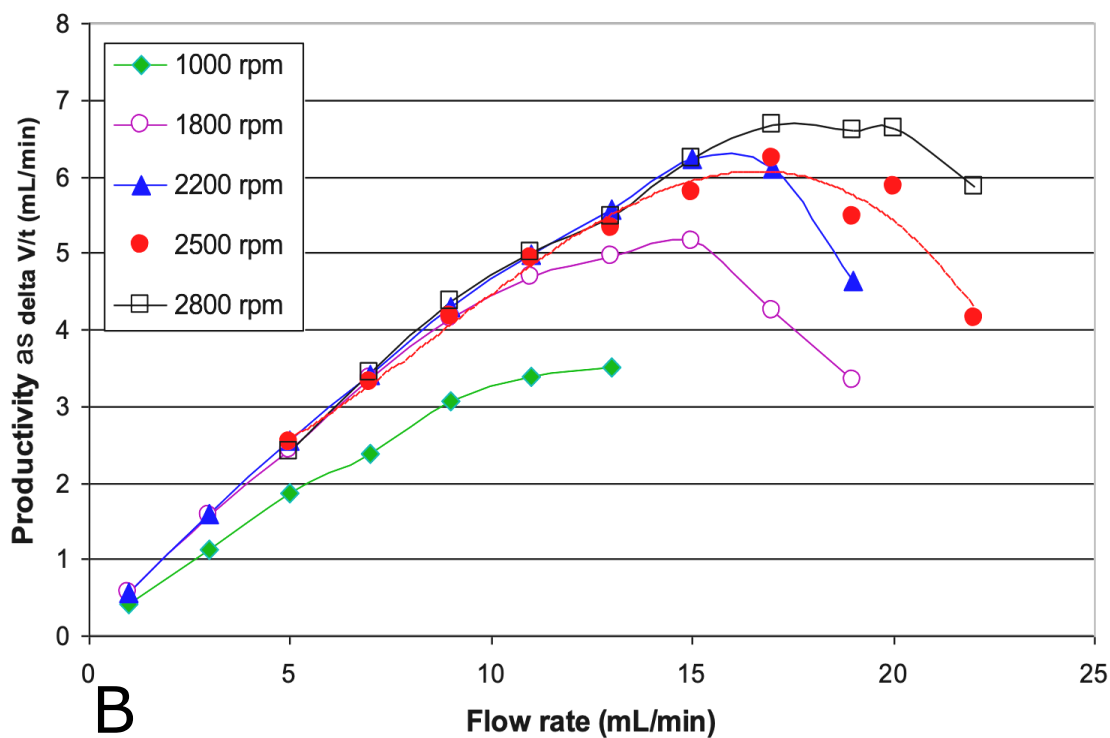
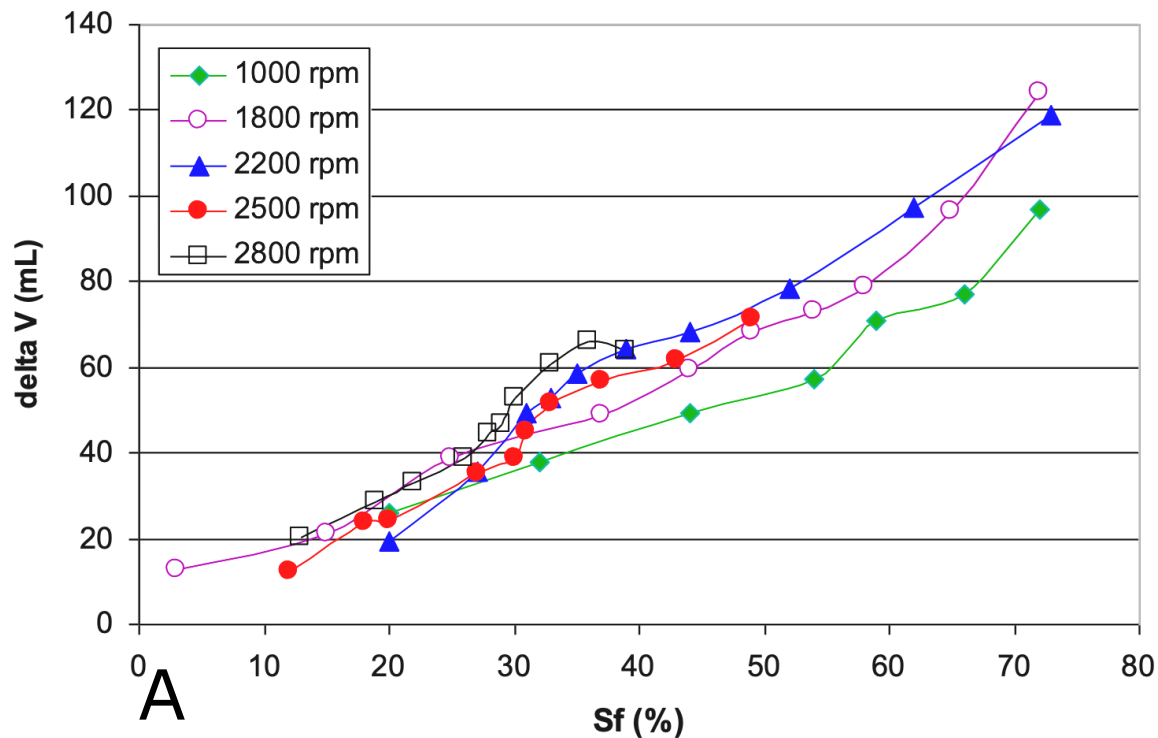
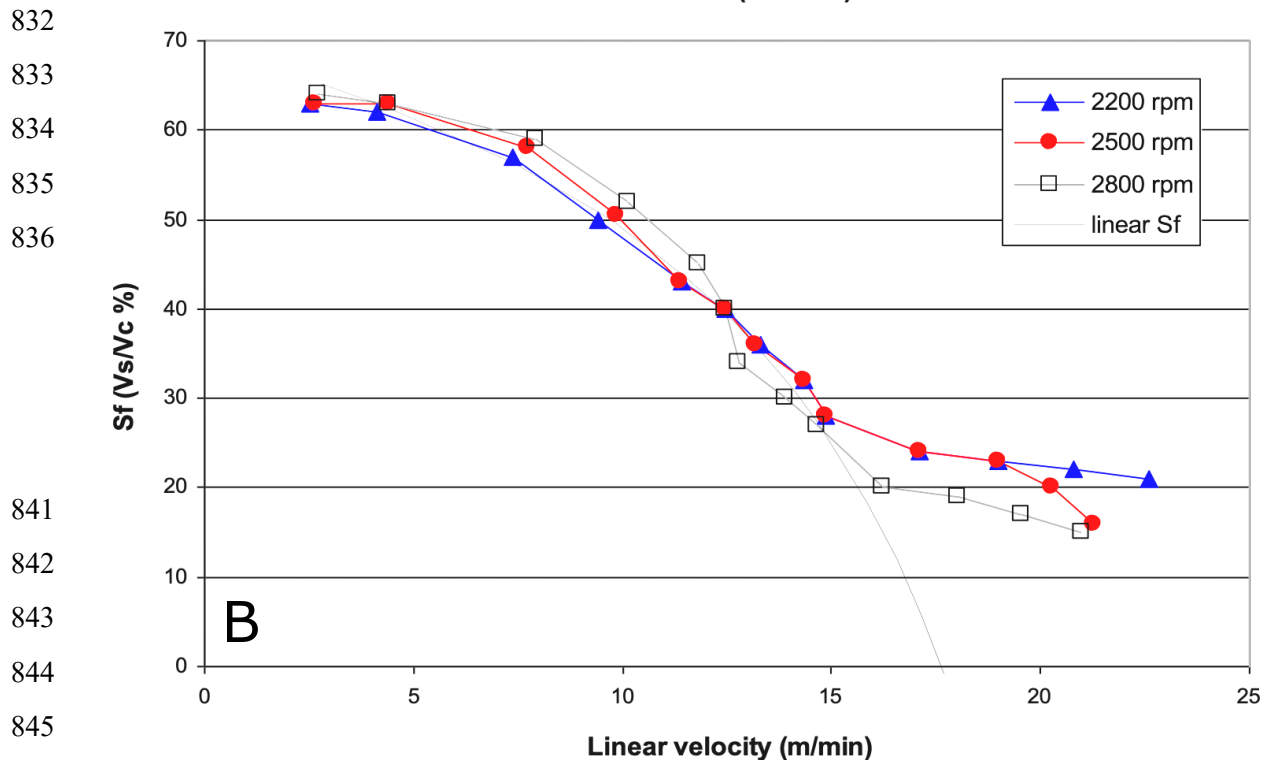
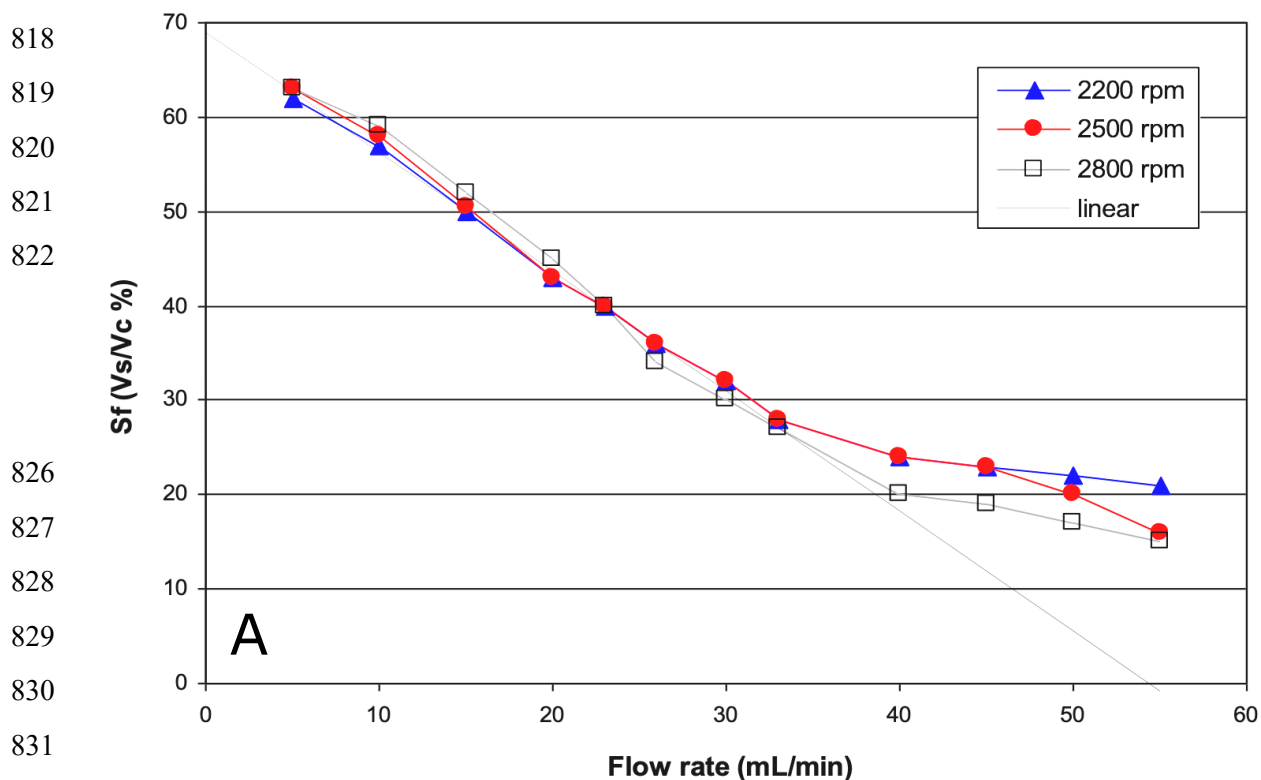


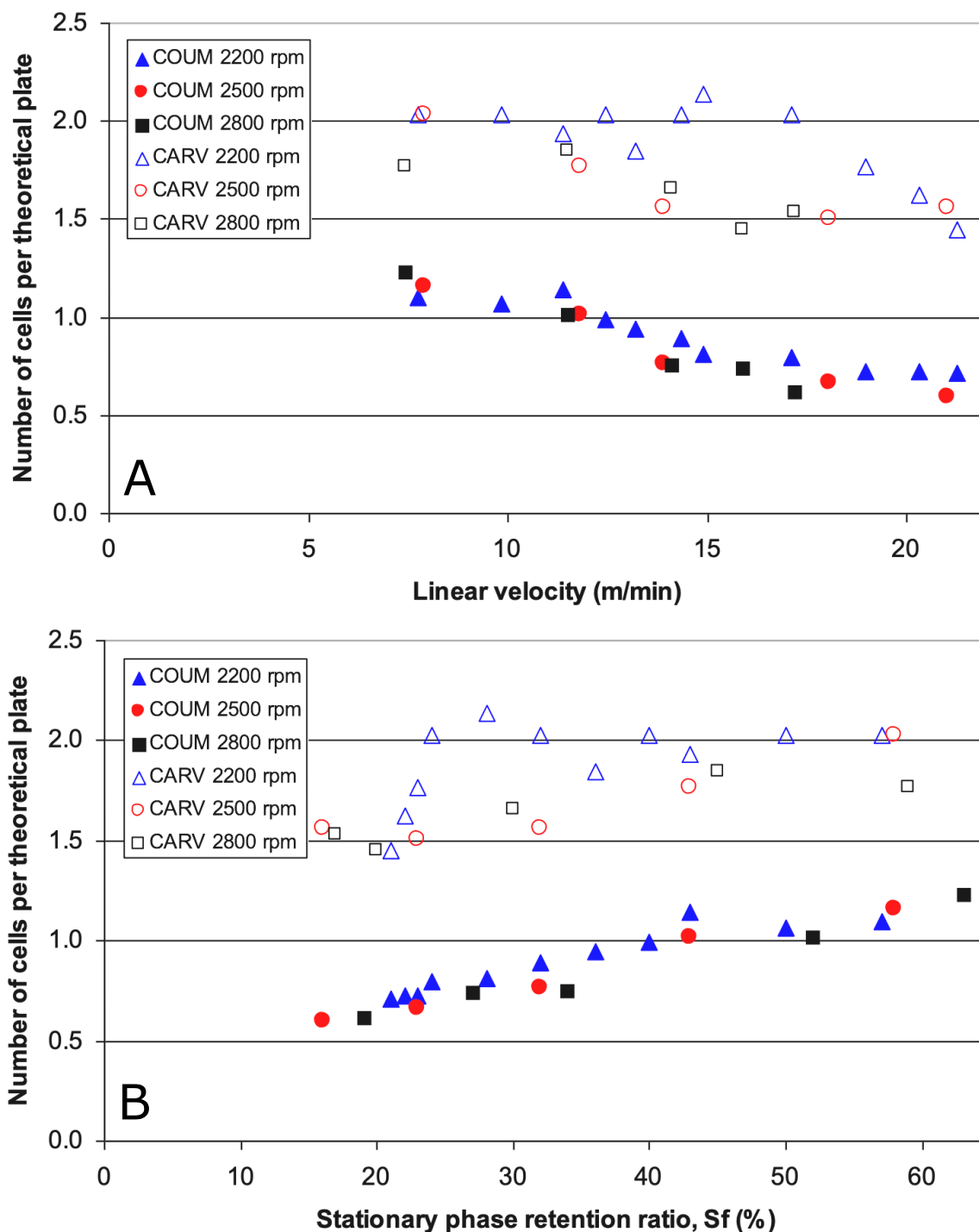
**Figure 4.** **A-** Free-space between coumarin and carvone peaks  $\Delta V$  as a function of  $S_f$ . **B-** Productivity expressed as the  $\Delta V/t$  ratio plotted versus mobile phase flow rate at different 30-mL rotor rotations.



847 **Figure 5.** Organic upper stationary phase retention (volume ratio),  $S_f$ , versus **A**-the  
848 aqueous mobile phase flow rate (mL/min) and **B**-the aqueous mobile phase velocity (m/min)  
849 at different 80-mL rotor rotations. The dotted lines correspond to the linear relation:  $S_f =$   
850  $69\% - 1.3 F$  (5A) transposed by eq. 4 in 5B. Compare with Fig. 2A and B for 30-mL rotor.

851

852  
853  
854  
855  
856  
857  
858  
859  
860  
861  
862  
863  
864  
865  
866  
867  
868  
869  
870  
871  
872  
873  
874  
875  
876  
877  
878  
879  
880



881 **Figure 6.** Coumarin (closed marks) and carvone (open marks) peak experimental  
882 efficiency expressed as the number of cells needed for one theoretical plate (NC/TP) plotted  
883 versus **A:** the mobile phase linear velocity and **B:** Sf, the volume ratio of stationary phase  
884 retained in the 80-mL CPC rotor spinning at indicated rotation speeds. System HEMWat o  
885 (AZ N) heptane/ethyl acetate/methanol/water 1:1:1:1 v/v, aqueous lower phase in the  
886 descending mode. Compare with Fig. 3 for 30-mL rotor.